Trop J Nat Prod Res, July 2025; 9(7): 3291 - 3296 ISSN 2616-0684 (Print)
ISSN 2616-0692 (Electronic)

Tropical Journal of Natural Product Research

Available online at https://www.tjnpr.org

Original Research Article

Verbascoside A as Potent Compound of *Cyperus rotundus* in Cytotoxic T Lymphocyte-Associated Antigen-4 (CTLA-4) Inhibition Based on Computational Model

Meddy Setiawan[1]*, Sulistyo M. Agustini[2], Mochamad Bahrudin[3], Noviana D. Lestari[4], Muhaimin Rifa'i[5]

[1]*Department of Internal Medicine, Faculty of Medicine, Muhammadiyah Malang University, St. Bendungan Sutami, Malang 65145, East Java, Indonesia*
[2]*Department of Pathology, Faculty of Medicine, Muhammadiyah Malang University, Malang 65145, East Java, Indonesia*
[3]*Department of Neurology, Faculty of Medicine, Muhammadiyah Malang University, Malang 65145, East Java, Indonesia*
[4]*Medical Education Study Program, Faculty of Medicine, Muhammadiyah Malang University, St. Bendungan Sutami, Malang 65145, East Java, Indonesia*
[5]*Biology Department, Faculty of Mathematics and Natural Sciences, Brawijaya University, Malang 65145, East Java, Indonesia*

ARTICLE INFO

Article history:
Received 25 January 2025
Revised 14 March 2025
Accepted 17 March 2025
Published online 01 August 2025

ABSTRACT

Cytotoxic T lymphocyte-associated antigen-4 (CTLA-4) regulation represents a significant therapeutic target in addressing regulatory T cell (Treg) dysfunction and enhancing immune responses within the tumor microenvironment (TME). This study aimed to evaluate the inhibitory effect of compounds of *Cyperus rotundus* against the immune checkpoint CTLA-4 *in silico*. Compounds from *Cyperus rotundus* tubers were identified by Liquid Chromatography-High Resolution Mass Spectrometry (LC-HRMS). The compounds' toxicity was predicted using Protox 3.0 web server. *In silico* study was performed using molecular docking and dynamics simulations of the compounds with CTLA-4 (PDB ID: 1I8L) protein using PyRx and YASARA softwares, respectively. Fourteen compounds were identified in *Cyperus rotundus* tubers. All compounds were classified as safe with LD_{50} value ranging from 740 to 26000 mg/kg. Molecular docking showed Verbascoside A and Maltopentaose as potential inhibitors of CTLA-4 with binding energies of -6.3 and -5.4 Kcal/mol, respectively. In the molecular dynamics simulation, RMSD values of all complexes exceeded 3 Å, indicating instability. However, the backbone RMSD and ligand conformation RMSD of CTLA4-Verbascoside A with values below 3 Å indicated more stability. Meanwhile, the CTLA4-maltopentaose complex exhibited higher RMSD value, indicating a change in the CTLA-4 protein structure when interacting with maltopentaose. Furthermore, the prediction of protein targets of maltopentaose and verbascoside A revealed potential direct and indirect target proteins related to cancer signaling pathways, namely; PI3K-Akt and estrogen signaling pathways. The ability of these compounds to modulate the TME-related CTLA-4 indicates their potential as anticancer drug candidates.

Keyword: Anti-cancer, *Cyperus rotundus*, Maltopentaose, Verbascoside A, Molecular Docking.

Introduction

Breast cancer including triple-negative breast cancer (TNBC) is a disease with a high prevalence rate and remains a challenge to treat.[1] One promising therapeutic approach in cancer treatment is immunotherapy, which aims to enhance the body's immune response against cancer cells. Immunotherapy is considered an effective therapy in cancer treatment, especially through the development of immune checkpoint inhibitors, such as Cytotoxic T-Lymphocyte-Associated Protein 4 (CTLA-4) inhibition.[2] CTLA-4 is a protein expressed on the surface of T cells, which plays an important role in regulating immune system activity. Activation of CTLA-4 leads to a decreased immune response to antigens, including tumor antigens, allowing cancer cells to escape immune system surveillance, so activation of CTLA-4 protein is often implicated in angiogenesis in cancer.[3]

*Corresponding author. E mail: meddy@umm.ac.id

Tel: +62 823 1350 6674

Citation: Setiawan M, Agustini SM, Bahrudin M, Lestari ND, Muhaimin Rifa'I M. Verbascoside A as Potent Compound of *Cyperus rotundus* in Cytotoxic T Lymphocyte-Associated Antigen-4 (CTLA-4) Inhibition Based on Computational Model. Trop J Nat Prod Res. 2025; 9(7): 3291 – 3296 https://doi.org/10.26538/tjnpr/v9i7.57

Official Journal of Natural Product Research Group, Faculty of Pharmacy, University of Benin, Benin City, Nigeria

CTLA-4 regulation in the tumor microenvironment (TME) is often associated with regulatory T cell (Treg) dysfunction, as well as increased immune cell infiltration. Treg cell activation in TME suppresses the activity of effector T cells (such as cytotoxic T cells and NK cells) that would otherwise attack tumor cells, creating a favorable environment for tumor growth.[4] In addition, Treg cells release immunosuppressive cytokines such as IL-10, TGF-β, and IL-35, which help reduce inflammation and inhibit the activity of other immune cells.[5] This allows the tumor to escape immune surveillance. CTLA-4 expressed by Treg cells also increases the expression of free PD-L1 on APCs.[6] This may inhibit the stimulatory activity of T cells by APCs and enhance the immunosuppressive effect. In addition, CTLA-4 activation in tumor cells can affect various signaling pathways such as MAPK, TGF-β, and TNF-α, which can modulate the immune microenvironment and affect the response to immunotherapy. Furthermore, CTLA-4 activation is also involved in various signaling pathways such as PI3K/AKT/mTOR and ERK1/2 signaling pathways that affect cancer cell proliferation.[7]

The use of herbal medicine such as *C. rotundus*in the mechanism of CTLA4 inhibition is one of the opportunities in cancer treatment, especially because of its bioactive compounds. *C. rotundus* is known to contain various bioactive compounds such as flavonoids, alkaloids, and terpenoids.[8] Furthermore, modern pharmacology has revealed the anti-cancer activity of *C. rotundus*, including inducing apoptosis and cell cycle arrest, as well as its potential in regulating inflammatory responses.[9] The mechanism of CTLA-4 inhibition by *C. rotundus* in regulating immune responses is still very unclear. The therapeutic potential of *C. rotundus* in regulating CTLA-4 activity in the TME is

still relatively limited. By targeting CTLA-4, *C. rotundus* bioactive compounds may reduce the activity of Treg. Therefore, this study aimed to evaluate the potential of bioactive compounds from *C. rotundus* in inhibiting CTLA-4 activity to attack cancer cells. By exploring the pharmacological mechanisms underlying the interaction between *C. rotundus* compounds and immune checkpoint pathways, this study seeks to provide a scientific basis for the development of novel plant-based adjunctive therapies in cancer treatment through a computational approach.

Materials and Methods

Collection and identification of plant material

C. rotundus (code: 240709.F.U.683) tubers were collected from Tirtomarto Village, Ampelgading, Malang, Indonesia (8°15'00.1"S; 112°53'00.6"E). The plant material was identified at East Java Provincial Government Health Office, UPT Materia Medica Batu with the voucher number 074/118/102.7/2017.

Extraction of plant material

The tubers were cut into small pieces and dried under the sun for two days. The dried tubers were finely ground into powder, and a total of 100 g powder was macerated with 500 mL of absolute ethanol at room temperature in an aluminum-covered flask to prevent light exposure and shaken on a rotary shaker at 120 rpm for 24 hours. The extract solution was stirred multiple times and allowed to settle, after which the supernatant was carefully separated. The liquid extract was filtered through a Whatman No. 1 filter paper, and the solvent was removed by rotary evaporation until a concentrated extract was obtained. Finally, the extract was stored at 4°C until further analysis.

LC-HRMS analysis

C. rotundus tuber extract were analyzed using Liquid Chromatography-High Resolution Mass Spectrometry (LC-HRMS) at the Laboratorium Riset Terpadu (LRT), Brawijaya University, Indonesia. Compounds with a BestMatch value exceeding 90% similarity were selected for computational analysis.[10]

In silico study

Ligand and protein preparation

The 3D structures of all the compounds were retrieved from the PubChem database in 3D-SDF file format and were analyzed using canonical SMILES.[11] The toxicity of the compounds was predicted using ProTox 3.0 web server to assess acute and organ toxicity profiles. The 3D structures of target protein: Cytotoxic T-lymphocyte-associated protein 4 (CTLA-4) was retrieved from Protein Data Bank (https://www.rcsb.org) with PDB ID: 1I8L (Table 1). Active site prediction was done by blind docking with the native ligand; 2-acetamido-2-deoxy-beta-D-glucopyranose (PubChem ID: 24139).

Table 1: Protein target preparation.

No	Protein	Native ligand/Inhibitor	Active site	Grid Center
1	CTLA-4 (PDB ID: 1I8L)	Alpha-D-mannopyranose (CID 185698)	TRP141, THR153, LEU139	Center = X: 8.7855; Y: 89.2589; Z: 184.2824 Dimensions (A) = X: 33.4123; Y: 30.1768; Z: 31.9980

Molecular docking and dynamics simulations

Molecular docking simulation was done using the AutoDock Vina integrated in PyRx software. The ligands (compounds from *C. rotundus* tubers) were docked with the target protein CTLA-4. Molecular docking results were presented in form of free energy change (ΔG), and visualized using Discovery Studio 2019 software.[12]

Molecular dynamics (MD) simulations were conducted using YASARA 23.4.25 software with the AMBER14 force field. The simulation environment was designed to mimic physiological conditions within human cells, including temperature (37°C), pH (7.4), salt concentration (0.9%), water density (0.997 g/mL), and pressure (1 atm). The 20 ns MD simulation was performed using the 'md_run' program, with data saved every 25 ps. The results were analyzed with the programs md_analyze for RMSD, md_analyze.res for RMSF, and md_bind energy for binding energy.[13]

The target proteins of the compounds Verbascoside A and Maltopentaose were obtained from the SWISS target prediction database (http://www.swisstargetprediction.ch/) or STITCH (http://stitch.embl.de/). For each compound, the five most significant target proteins were selected. Indirect targets of each active compound were obtained from the STRING web server (https://string-db.org/) by inputting the target proteins. All results obtained were merged and visualized using Cytoscape 3.10.3 software.[14]

All proteins obtained from the PPI network construction were inputted into the DAVID webserver (https://davidbioinformatics.nih.gov/). Functional annotation was performed using Gene Ontology and KEGG pathway databases, focusing on biological mechanisms related to apoptosis, proliferation, and cell migration.[15]

Results and Discussion

Fourteen (14) bioactive compounds were identified from the LC-HRMS analysis of *C. rotundus* tuber (Table 2). The toxicity of the compounds were predicted using ProTox 3.0. web server. From the toxicity prediction, all the compounds belong to class IV – V toxicity categories, with LD_{50} value ranging from 740 to 26000 mg/kg. The lower limit of this range (740 mg/kg) suggests that the compounds are relatively safe when consumed at moderate doses by humans, implying that very high doses would be required to cause toxic effect. This reinforces the claim that these compounds are relatively safe when consumed in normal therapeutic doses. However, the toxicity prediction revealed that some of the compounds have the potential to affect specific organs. L-Aspartic acid, (-)-Caryophyllene oxide, and Maleamate were predicted as the safest compounds with non-toxic effects on organs. On the other hand, Guanine was shown to be toxic to three organs/systems: the liver, nervous system, and respiratory system. Nootkatone, in particular, requires close attention due to its predicted toxicity to the liver, nervous system, kidneys, and respiratory system. This information on organ-specific toxicity can serve as an important screening tool for assessing the safety of these compounds for potential therapeutic applications. The potential toxicity of certain compounds highlights the importance of monitoring organ function and identifying underlying conditions in patients before using these compounds as medicine. Moreover, prolonged use or high doses could increase the risk of organ toxicity, making it crucial to consider these factors during treatment planning. Therefore, identifying patients' pre-existing conditions and potential organ toxicity should be part of the screening process when considering these compounds as drug candidates.[16]

Molecular docking was performed on all of *C. rotundus* compounds to analyze the interaction of each compound with CLTA-4 protein. The whole complex binding affinity values are shown in Table 3. Seven compounds, namely Verbascoside A (-6.3 Kcal/mol), Maltopentaose (-5.4 Kcal/mol), 1-Nitro-2-phenoxybenzene (-5.1 Kcal/mol), (-)-Caryophyllene oxide (-5.1 Kcal/mol), Phthalic acid (-5 Kcal/mol), Nootkatone (-5 Kcal/mol), and Guanine (-4.9 Kcal/mol), have smaller binding affinity values than the inhibitor compound alpha-D-mannopyranose (-4.8 Kcal/mol) (Table 4). This indicates that the seven compounds are better competitive inhibitors than the native inhibitor. Smaller binding affinity values indicate stronger and more stable protein and ligand interactions.[17] Verbascoside A and maltopentaose were selected as the most promising compounds, and were used in the molecular dynamics study. The molecular docking interaction results of Verbascoside A and Maltopentaose showed that both compounds potentially bind to the same active site as the native ligand.

Furthermore, Verbascoside A showed the potential of affecting the protein structure as indicated by the difference in the shape of the resulting protein when compared to the native ligand. It can be assumed that Verbascoside A is a strong inhibitor drug candidate against the CTLA-4 protein structure, supported by the binding energy value.

The results of the molecular dynamics interaction analysis showed that the ligands have the potential to significantly affect the structure of the protein complex. Verbascoside A and Maltopentaose showed a high degree of stability by continuous interaction at the protein active site throughout the duration of the simulation (20 ns). In contrast, the native ligand showed a shift in position at the binding site, indicating a potential decrease in affinity or stability of the interaction with the protein. These findings underscore the ability of Verbascoside A and Maltopentaose ligands to maintain specific interactions with the active site, potentially affecting the biological activity of the protein within 20 ns (Figure 1).

Table 2: Bioactive compounds in *C. rotundus* from LC-HRMS analysis.

No	Name	Formula	MW (g/mol)	RT [min]	Area (Max.)	mzCloud Best Match	CID
1	Bis(2-ethylhexyl) phthalate	$C_{24}H_{38}O_4$	390.6	23.381	337,706.05	98.6	8343
2	Verbascoside A	$C_{31}H_{40}O_{16}$	668.6	1.031	9,835,989.92	98.1	15736674
3	Maltopentaose	$C_{30}H_{52}O_{26}$	828.7	1.065	195,952.82	96.6	124005
4	n-Pentyl isopentyl phthalate	$C_{18}H_{26}O_4$	306.4	13.919	1,436,938.92	95.6	71307505
5	L-Homocysteine	$C_4H_9NO_2S$	135.19	7.499	352,685.86	95.3	91552
6	L(+)-Ornithine	$C_5H_{12}N_2O_2$	132.16	1.129	124,309.48	94.6	6262
7	L-Aspartic acid	$C_4H_7NO_4$	133.10	0.974	648,504.68	94.3	5960
8	(-)-Caryophyllene oxide	$C_{15}H_{24}O$	220.35	18.739	836,643.56	94.2	1742210
9	Choline	$C_5H_{14}NO_+$	104.17	1.181	434,793.75	94	305
10	Guanine	$C_5H_5N_5O$	151.13	1.475	106,192.19	93.9	135398634
11	1-Nitro-2-phenoxybenzene	$C_{12}H_9NO_3$	215.20	1.081	358,141.28	93.4	16661
12	Nootkatone	$C_{14}H_{14}N_2O_3S_2$	322.4	17.91	240,279.60	93	2813732
13	Phthalic acid	$C_8H_6O_4$	166.13	23.386	3,122,162.26	92.4	1017
14	Maleamate	$C_4H_5NO_3$	115.09	0.96	182,412.60	91.2	5280451

Table 3: Toxicity prediction of bioactive compounds from *C. rotundus*

No.	Compound Name	Predicted LD_{50} (mg/kg)	Tox Class	Probability Organ toxicity ($^+$Activ)				
				Hepa	Neuro	Nephro	Respi	Cardio
1	Bis(2-ethylhexyl) phthalate	1340	4	0.82	0.81	0.57+	0.98	0.79
2	Verbascoside A	5000	5	0.84	0.86	0.56+	0.52+	0.57
3	Maltopentaose	10000	6	0.93	0.92	0.81+	0.57	0.96+
4	n-Pentyl isopentyl phthalate	26000	6	0.76	0.83	0.55+	0.99	0.74
5	L-Homocysteine	6700	5	0.93	0.7	0.55	0.5+	0.86+
6	L(+)-Ornithine	5000	5	0.95	0.73	0.54	0.69+	0.95+
7	L-Aspartic acid	923	4	0.83	0.82	0.56	0.84	0.65
8	(-)-Caryophyllene oxide	5000	5	0.8	0.57	0.86	0.65	0.84
9	Choline	1391	4	0.94	0.55+	0.82	0.85+	0.69
10	Guanine	800	3	0.51+	0.75+	0.57	0.5+	0.88
11	1-Nitro-2-phenoxybenzene	740	4	0.6+	0.68	0.62	0.87	0.51
12	Nootkatone	1000	4	0.54+	0.55+	0.58+	0.7+	0.78
13	Phthalic acid	2530	5	0.65	0.85	0.65+	0.78+	0.79
14	Maleamate	2400	4	076	0.69	0.51	0.74	0.59

Note: ($^+$) = Probability organ toxicity active, (Non $^+$) = Probability organ toxicity inactive

The results of molecular dynamics analysis showed changes in amino acid residues involved in the interaction of Maltopentaose ligand with protein when switching from molecular docking to molecular dynamics simulation for 20 ns. For van der Waals interaction, the residues involved in molecular docking include HIS138, LEU139, THR154, VAL155, TRP141, LEU148, SER140, ILE151, and ASN152. However, during molecular dynamics simulations, these residues changed to VAL166 and SER140, reflecting the presence of protein-ligand structural dynamics. In the interaction through conventional hydrogen bonding, residues ALA150, THR153, and GLU147 play a role in molecular docking, while in molecular dynamics, the residues involved became PRO137, LEU139, and VAL155. In addition, in the carbon hydrogen bond category, the residue ASN149 in molecular docking changed during molecular dynamics simulation to HIS138, THR154, and THR153. These changes in the residues involved indicated the flexibility of the protein structure in binding to the ligand during simulation, which may affect the stability and affinity of the protein-ligand complex interaction.

The results of the interaction analysis of Verbascoside A with proteins showed differences in the residues involved between molecular docking and molecular dynamics simulations for 20 ns. In the van der Waals interaction, molecular docking identified residues THR110, PRO111, SER112, GLN193, SER114, PHE195, THR194, and THR199 as the residues involved (Table 5). However, during molecular dynamics simulations, these residues changed to THR194, GLU143, PHE180, GLY145, ASN192, LEU183, and ARG190, reflecting the structural adaptation of the protein to the ligand in a dynamic environment. In

conventional hydrogen bonding, residues ILE113, ASN196, and ASN198 were detected during docking, whereas in molecular dynamics simulations, only ASN144 played a role. Interactions through carbon hydrogen bonding showed the involvement of residues SER179 and ASN196 at the docking stage, while these interactions were not identified during molecular dynamics simulations. In contrast, hydrophobic interactions in molecular docking only involved residue TRP197, which was changed to MET181 and LEU142 during simulation. These changes in interaction patterns highlight the dynamic flexibility of protein and ligand structures in simulations, which cannot be completely revealed through static docking methods.[18]

The analysis of native ligand (inhibitor) interaction with protein showed significant residue differences between molecular docking and molecular dynamics simulation. In the van der Waals interaction, molecular docking identified residues ILE151, GLU147, and LEU139 as the residues that played a role. However, during the molecular dynamics simulations, these residues changed to LYS86, HIS18, and VAL20, reflecting the changes in the interaction caused by the flexibility of the protein and ligand structures in the dynamic environment. In conventional hydrogen bonding, residues ALA150, LEU148, TRP141, SER168, and THR153 were detected during docking, whereas in molecular dynamics simulations the residues involved changed to ASN19, SER21, and GLU24. Meanwhile, the interaction through carbon hydrogen bonds which in molecular docking involved residue ASN149, was not found during molecular dynamics simulation. This difference suggests that molecular dynamics simulation is able to reveal more realistic dynamics and interaction patterns compared to the static docking approach.[19]

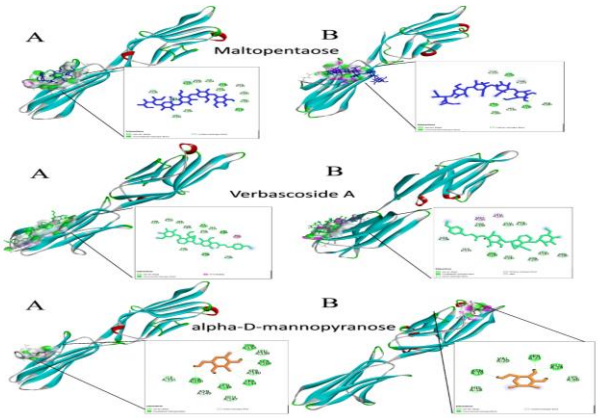

Figure 1: Bioinfomatic prediction of *C. rotundus*. (A) 3D Molecular docking simulation, (B) 3D Molecular dynamic simulation

Table 4: Molecular docking simulation results

Ligand	Binding Affinity Kcal/mol
Verbascoside A	-6.3
Maltopentaose	-5.4
1-Nitro-2-phenoxybenzene	-5.1
(-)-Caryophyllene oxide	-5.1
Phthalic acid	-5
Nootkatone	-5
Guanine	-4.9
Bis(2-ethylhexyl) phthalate	-4.7
n-Pentyl isopentyl phthalate	-4.6
Maleamate	-4
L-Aspartic acid	-4
L(+)-Ornithine	-3.6
L-Homocysteine	-3.3
Choline	-3.1
alpha-D-mannopyranose/Inhibitor	-4.8

Molecular Dynamics Simulation Results

Molecular dynamics simulation was used to analyze the stability and conformation of CTLA4 protein interacting with Maltopentaose and Verbascoside A, using the parameters; Root Mean Square Deviation (RMSD), RMSD backbone, RMSD ligand conformation, RMSD ligand movement, Radius of gyration (Rg), number of hydrogen bonds, Root Mean Square Fluctuation (RMSF), and binding energy. The simulation results can be seen in Figure 2.

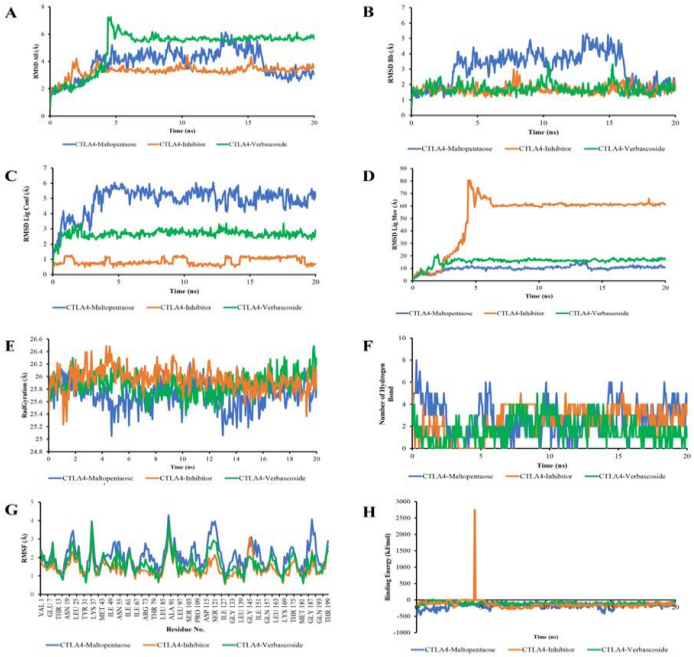

Figure 2: Molecular dynamics simulation of CTLA protein complex with maltopentaose and verbascoside ligands. (A) Values of RMSD All, (B) RMSD backbone, (C) RMSD ligand conformation, (D) RMSD Ligand movement, (E) Radius of gyration (F) Number of hydrogen bonds (G) RMSF, (H) Binding energy

RMSD is used to measure the structural changes in the protein backbone during simulation and assess its conformational stability. The smaller the RMSD value, the more stable the protein structure.[20] The protein structure is considered stable if it has RMSD value is below 3 Å.[21] All the protein-ligand complexes appeared less stable because the RMSD values fluctuated slightly above 3 Å (Figure 2A). However, the CTLA4-maltopentaose complex was slightly more stable, almost close to the CTLA4 complexed with the native ligand. The backbone RMSD (Figure 2B) and ligand conformation RMSD (Figure 2C) of CTLA4-Verbascoside A with values below 3 Å indicated fluctuation in stability during the simulation. Meanwhile, the CTLA4-maltopentaose complex exhibited an increase in the RMSD value, indicating a change in the CTLA4 protein structure when interacting with Maltopentaose. The RMSD value of ligand movement in the CTLA4 complex that binds to the inhibitor ligand in the time range of 0-6 ns increased sharply, then stabilized from 7 ns until the end of the simulation. On the other hand, CTLA4 complexed with Maltopentaose and Verbascoside Ahad stable values from the beginning to the end of the simulation (Figure 2D). Radius of gyration is used to describe the compactness of protein structure.[22] The Rg values of all complexes in this study were stable, indicating that there were no significant conformational changes in the protein structure after interacting with the ligands (Figure 2E).

The CTLA4 complexes when interacting with Maltopentaose and Verbascoside A, contained hydrogen bonds comparable to the native ligand, meaning that the protein-ligand complexes were stable. The greater number of hydrogen bonds, the greater the strengthen the protein-ligand interaction.[23] RMSF assesses protein conformational changes based on amino acid residue fluctuations.[24] All complexes at

amino acid residues LYS6 and LYS89 were unstable, showing fluctuations during the simulation, and the values were more than 3 Å. However, the RMSF for the maltopentaose complex was found to fluctuate more with values above 3 Å than the other complexes. The binding energy values of Maltopentaose and Verbascoside A complexes had similar stability to the native ligand. However, the binding energy value of the inhibitor at 4.5 ns experienced instability, reaching about 2738 kJ/mol.

Table 5: Residues ligand-protein interaction.

Compound	Types of interactions	Residue	
		Molecular docking	Molecular dynamic
Maltopentaose	Van der waals	HIS138, LEU139, THR154, VAL155, TRP141, LEU148, SER140, ILE151, ASN152	VAL166, SER140
	Conventional Hydrogen	ALA150, THR153, GLU147,	PRO137, LEU139, VAL155
	Carbon Hydrogen	ASN149,	HIS138, THR154, THR153
Verbascoside A	Van der Waals	THR110, PRO111, SER112, GLN193, SER114, PHE195, THR194, THR199	THR194, GLU143, PHE180, GLY145, ASN192, LEU183, ARG190
	Conventional Hydrogen Bond	ILE113, ASN196, ASN198	ASN144
	Carbon Hydrogen		SER179, ASN196
	Hydrophobic	TRP197	MET181, LEU142
	Van der Waals	ILE151, GLU147, LEU139	LYS86, HIS18, VAL20
Inhibitor	Conventional Hydrogen Bond	ALA150, LEU148, TRP141, SER168, THR153	ASN19, SER21, GLU24
	Carbon Hydrogen	ASN149	

Furthermore, the analysis showed that the compounds Maltopentaose and Verbascoside A target important proteins in the apoptosis, proliferation, and migration of breast cancer cells. The PPI network is presented in Figure 3A, which shows the interaction network of the target proteins of the two compounds with other proteins. The role of these target proteins in the signaling pathway is shown in Figure 3B. These results showed that the target proteins of Maltopentaose and Verbascoside A target proteins related to signaling pathways in cancer, namely; the PI3K-Akt signaling pathway and the estrogen signaling pathway. These pathways are critical in regulating cancer cell proliferation and survival. Additionally, pathways directly influencing cell migration, such as those involving cell adhesion molecules and the regulation of the actin cytoskeleton, were identified. Functional annotation using the Gene Ontology database further supports the role of these target proteins in cancer progression.[25]

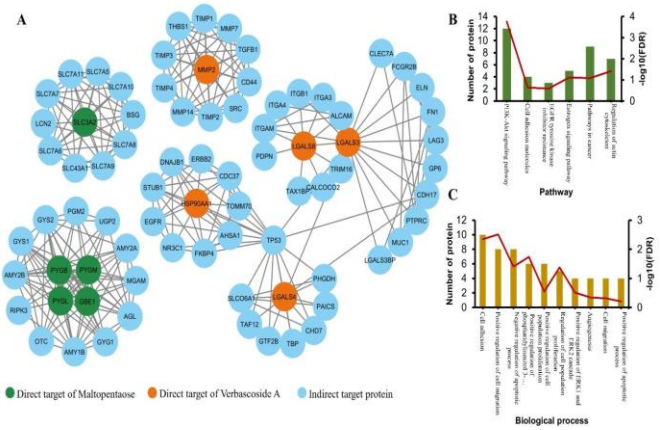

Figure 3: Protein interaction prediction of potential compounds. (A) PPI network, (B) functional annotation based on database KEGG pathway, (C) Gene ontology

Conclusion

The therapeutic potential of *C. rotundus* in regulating CTLA-4 activity within the TME remains a relatively unexplored yet promising domain. By targeting CTLA-4, the bioactive compounds of *C. rotundus* could enhance T-cell-mediated antitumor immunity while mitigating the suppressive effects of Treg. The toxicity analysis indicated that the compounds of *C. rotundus* are classified as safe for consumption based on Protox Toxicity prediction. Based on molecular docking and molecular dynamics, Verbascoside A showed stronger binding affinity and more stable simulated bindings compared to the other compounds and the native ligand, while Maltopentaose showed more fluctuations. Furthermore, the ability of these compounds to modulate other hallmarks of the TME, such as angiogenesis and oxidative stress, positions *C. rotundus* as a multifaceted candidate for integrative cancer therapy. Future pre-clinical trials *in vivo* and *in vitro* could investigate their efficacy for cancer treatment.

Conflict of Interest

The authors declare no conflicts of interest.

Authors' Declaration

The authors hereby declare that the work presented in this article are original and that any liability for claims relating to the content of this article will be borne by them.

Acknowledgments

The authors gratefully thank the University of Muhammadiyah Malang and Directorate of Research and Community Service (DRPM) for supporting this study with Block grand number 109/E5/PG.02.00.PL/2024. The authors would like to thank the Widodo and Muhaimin Research Team for sharing the computational software facility in the Department of Biology, Universitas Brawijaya.

References

1. Oladeru O, Rajack F, Esnakula A, Naab TJ, Kanaan Y, Ricks-Santi L. Beyond triple-negative: high prevalence of quadruple-negative breast cancer in African Americans. Biomed. 2024; 12(7): 1522. Doi: 10.3390/biomedicines12071522
2. Shiravand Y, Khodadadi F, Kashani SMA, Hosseini-Fard SR, Hosseini S, Sadeghirad H, Ladwa R, O'Byrne K, Kulasinghe A. Immune checkpoint inhibitors in cancer therapy. Curr Oncol. 2022; 29(5): 3044-3060. Doi: 10.3390/curroncol29050247
3. Buchbinder EI and Desai A. CTLA-4 and PD-1 pathways: similarities, differences, and implications of their inhibition.

Am J Clin Oncol. 2016; 39(1): 98-106. Doi: 10.1097/COC.0000000000000239
4. Rocamora-Reverte L, Melzer FL, Würzner R, Weinberger B. The complex role of regulatory T cells in immunity and aging. Front Immunol. 2021; 11:616949. Doi: 10.3389/fimmu.2020.616949
5. Liu Z, Zhou J, Wu S, Chen Z, Wu S, Chen L, Zhu X, Li Z. Why Treg should be the focus of cancer immunotherapy: the latest thought. Biomed Pharmacother. 2023; 168: 115142. Doi: 10.1016/j.biopha.2023.115142
6. Tekguc M, Wing JB, Osaki M, Long J, Sakaguchi S. Treg-expressed CTLA-4 depletes CD80/CD86 by trogocytosis, releasing free PD-L1 on antigen-presenting cells. Proc Natl Acad Sci. 2021; 118(30): e2023739118. Doi: 10.1073/pnas.2023739118
7. Navarrete-Bernal MGC, Cervantes-Badillo MG, Martínez-Herrera JF, Lara-Torres CO, Gerson-Cwilich R, Zentella-Dehesa A, Ibarra-Sánchez MDJ, Esparza-López J, Montesinos JJ, Cortés-Morales VA, Osorio-Pérez D, Villegas-Osorno DA, Reyes-Sánchez E, Salazar-Sojo P, Tallabs-Utrilla LF, Romero-Córdoba S, Rocha-Zavaleta L. Biological landscape of triple negative breast cancers expressing CTLA-4. Front Oncol. 2020; 10: 1206. Doi: 10.3389/fonc.2020.01206
8. Konsue A and Taepongsorat L. Phytochemical Screening and Antioxidant Activity of Longevity Remedy from National Thai Traditional Medicine Scripture (Formulary Special Edition). Trop J Nat Prod Res. 2022; 6(6): 868-871. Doi: 10.26538/tjnpr/v6i6.6
9. Lin CH, Peng SF, Chueh FS, Cheng ZY, Kuo CL, Chung JG. The ethanol crude extraction of *Cyperus rotundus* regulates apoptosis-associated gene expression in HeLa human cervical carcinoma cells *in vitro*. Anticancer Res. 2019; 39(7): 3697-3709. Doi: 10.21873/anticanres.13518
10. Setiawan M, Agustini SM, Patmawati, Lestari ND. In silico approach for predicting the bioactive compound of *Cyperus rotundus* to inhibit NF-kB and iNOS signaling pathways. Braz J Biol. 2024; 84: e278323. Doi: 10.1590/1519-6984.278323
11. Banerjee P, Kemmler E, Dunkel M, Preissner R. ProTox 3.0: a webserver for the prediction of toxicity of chemicals. Nucleic Acids Res. 2024; 52(W1): W513-W520. Doi: 10.1093/nar/gkae303
12. Dwijayanti DR, Widyananda MH, Hermanto FE, Soewondo A, Afiyanti M, Widodo N. Revealing the anti-inflammatory activity of *Euphorbia hirta* extract: transcriptomic and nitric oxide production analysis in LPS-Induced RAW 264.7 cells. Food Agric Immunol. 2024; 35(1): 2351360. Doi: 10.1080/09540105.2024.2351360
13. Nafisah W, Fatchiyah F, Widyananda MH, Christina YI, Rifa'i M, Widodo N, Djati MS. Potential of bioactive compound of *Cyperus rotundus* L. rhizome extract as inhibitor of PD-L1/PD-1 interaction: an *in silico* study. Agric Nat Resour. 2022; 56(4): 751-760. Doi: 10.34044/j.anres.2022.56.4.09
14. Lestari ND, Adharini WI, Widodo W, Rahayu S, Tsuboi H, Jatmiko YD, Rifa'i M. Anti-inflammatory evaluation of Moringa-Albumin combination in inhibiting IFN-γ and TNF-α expression in diabetic mouse model. Res J Pharm Technol. 2022; 15(2): 628-632. Doi: 10.52711/0974-360X.2022.00103
15. Chen W, Han Y, Chen Y, Liu X, Liang H, Wang C, Khan MZ. Potential Candidate Genes Associated with Litter Size in Goats: A Review. Animals. 2025; 15(1): 82. Doi: 10.3390/ani15010082
16. Blomme EAG and Will Y. Toxicology strategies for drug discovery: present and future. Chem Res Toxicol. 2016; 29(4): 473-504. Doi: 10.1021/acs.chemrestox.5b00407
17. Spassov DS. Binding affinity determination in drug design: insights from lock and key, induced fit, conformational selection, and inhibitor trapping models. Int J Mol Sci. 2024; 25(13):7124. Doi: 10.3390/ijms25137124
18. Adcock SA and McCammon JA. Molecular dynamics: survey of methods for simulating the activity of proteins. Chem Rev. 2006; 106(5): 1589-1615. Doi: 10.1021/cr040426m
19. Salmaso V and Moro S. Bridging molecular docking to molecular dynamics in exploring ligand-protein recognition process: an overview. Front Pharmacol. 2018; 9: 923. Doi: 10.3389/fphar.2018.00923
20. Aier I, Varadwaj PK, Raj U. Structural insights into conformational stability of both wild-type and mutant EZH2 receptor. Sci Rep. 2016; 6(1):34984. Doi: 10.1038/srep34984
21. Opo FADM, Rahman MM, Ahammad F, Ahmed I, Bhuiyan MA, Asiri AM. Structure based pharmacophore modeling, virtual screening, molecular docking and ADMET approaches for identification of natural anti-cancer agents targeting XIAP protein. Sci Rep. 2021; 11(1):4049. Doi: 10.1038/s41598-021-83626-x
22. Rampogu S, Lee G, Park JS, Lee KW, Kim MO. Molecular docking and molecular dynamics simulations discover curcumin analogue as a plausible dual inhibitor for SARS-CoV-2. Int J Mol Sci. 2022; 23(3): 1771. Doi: 10.3390/ijms23031771
23. Halder SK, Sultana I, Shuvo MN, Shil A, Himel MK, Hasan MdA, Shawan MMAK. *In silico* identification and analysis of potentially bioactive antiviral phytochemicals against SARS-CoV-2: a molecular docking and dynamics simulation approach. BioMed Res Int. 2023; 2023(1):5469258. Doi: 10.1155/2023/5469258
24. Das R, Bhattarai A, Karn R, Tamang B. Computational investigations of potential inhibitors of monkeypox virus envelope protein E8 through molecular docking and molecular dynamics simulations. Sci Rep. 2024; 14(1):19585. Doi: 10.1038/s41598-024-70433-3
25. Qasqas LM, Khleifat K, Shadid KA, Qaralleh H, Alqaraleh M. The Impact of Amphimedon chloros Ethyl Acetate Extract on MDA-MB-231 Cell Lines' Expression of Bax, Cyclin D, Caspase 3, P21, C-myc, and Bcl2: Mechanism of inhibition of the Growth of Cancer Cells. Trop J Nat Prod Res. 2024; 8(9):8307-8313. Doi: 10.26538/tjnpr/v8i9.9